Since January 2020 Elsevier has created a COVID-19 resource centre with free information in English and Mandarin on the novel coronavirus COVID-19. The COVID-19 resource centre is hosted on Elsevier Connect, the company's public news and information website.

Analytica Chimica Acta 1221 (2022) 340120

Contents lists available at ScienceDirect

Analytica Chimica Acta

journal homepage: www.elsevier.com/locate/aca

Ultrasensitive SARS-CoV-2 diagnosis by CRISPR-based screen-printed carbon electrode

Lina Wu [a,b,*,1], Xinjie Wang [c,1], Chengyuan Wu [a], Xizhong Cao [d], Taishan Tang [d], He Huang [a,e,**], Xingxu Huang [b,***]

[a] School of Food Science and Pharmaceutical Engineering, Nanjing Normal University, Nanjing, 210023, PR China
[b] Zhejiang Laboratory, Hangzhou, 311100, PR China
[c] Shenzhen Branch, Guangdong Laboratory of Lingnan Modern Agriculture, Genome Analysis Laboratory of the Ministry of Agriculture and Rural Affairs, Agricultural Genomics Institute at Shenzhen, Chinese Academy of Agricultural Sciences, Shenzhen, 518120, PR China
[d] Animal, Plant and Food Inspection Center of Nanjing Customs District, Nanjing, 210023, PR China
[e] College of Pharmaceutical Science, Nanjing Tech University, Nanjing, 211816, PR China

HIGHLIGHTS

- The ssDNA reporter randomly distributed on the electrode could be cleavaged by activated Cas12a protein as well as the ssDNA fixed upright on the surface of the electrode which could greatly shorten the time of ssDNA reporter immobilization.
- CRISPR-SPCE enabled ultra-sensitivity SARS-CoV-2 detection, with a detection limit as low as 0.27 copy/μL.
- CRISPR-screen-printed carbon electrode system is fast, high specific and low cost, thus providing a simple and faster path way for SARS-CoV-2 detection.

GRAPHICAL ABSTRACT

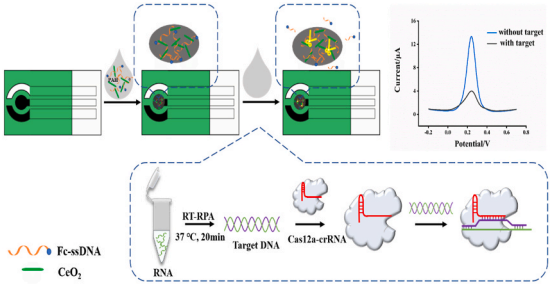

ARTICLE INFO

Keywords:
Screen-printed carbon electrode
CRISPR/Cas12a
SARS-CoV-2
CeO_2 nanorods
Detection

ABSTRACT

Early and accurate diagnosis of SARS-CoV-2 was crucial for COVID-19 control and urgently required ultrasensitive and rapid detection methods. CRISPR-based detection systems have great potential for rapid SARS-CoV-2 detection, but detecting ultra-low viral loads remains technically challenging. Here, we report an ultrasensitive CRISPR/Cas12a-based electrochemical detection system with an electrochemical biosensor, dubbed CRISPR-SPCE, in which the CRISPR ssDNA reporter was immobilized onto a screen-printed carbon electrode. Electrochemical signals are detected due to CRISPR cleavage, giving enhanced detection sensitivity. CRISPR-SPCE enables ultrasensitive SARS-CoV-2 detection, reaching as few as 0.27 copies μL^{-1}. Moreover, CRISPR-SPCE is also highly specific and inexpensive, providing a fast and simple SARS-CoV-2 assay.

* Corresponding author. School of Food Science and Pharmaceutical Engineering, Nanjing Normal University, Nanjing, 210023, PR China.
** Corresponding author. School of Food Science and Pharmaceutical Engineering, Nanjing Normal University, Nanjing, 210023, PR China.
*** Corresponding author.
E-mail addresses: wuln@njnu.edu.cn (L. Wu), huangh@njnu.edu.cn (H. Huang), xingxuhuang@nju.edu.cn (X. Huang).
[1] These authors have contributed equally to this work.

https://doi.org/10.1016/j.aca.2022.340120
Received 7 May 2022; Received in revised form 13 June 2022; Accepted 22 June 2022
Available online 2 July 2022

1. Introduction

The fast-spreading severe acute respiratory syndrome coronavirus-2 (SARS-CoV-2) is endangering human health and the world's economies, lowering production and limiting travel [1–3]. The detection of SARS-CoV-2 is crucial for isolating infected individuals and preventing the virus from spreading in the general population [4,5]. Digital PCR and real-time reverse transcription PCR have been applied for SARS-CoV-2 detection [6–8]. However, these methods require special instruments, skilled personnel and are time-consuming [9–11]. Recently, new methods requiring no particular instrumentation have been developed based on the CRISPR/Cas system (clustered regularly interspaced short palindromic repeats and CRISPR-associated protein) [12,13].

CRISPR/Cas system, which normally plays the role of a bacterial immune systems [14,15], has been developed into powerful tools for genome editing [16,17], genome imaging [18], cell imaging [19–21], and disease treatment [22–24]. The CRISPR/Cas system is also a promising platform for next-generation molecular detection technologies with high sensitivity and specificity that require no special instrumentation [25,26]. The *trans*-cleavage activity of Cas effector proteins (such as Cas12, Cas13, Cas14, etc.) [27–30] combined with signal amplification [31,32] has achieved ultrasensitive, specific and cheaper DNA or RNA detection in applications such as SHERLOCK (specific high-sensitivity enzymatic reporter unlocking) and DETECTR DNA (endonuclease-targeted CRISPR trans reporter) [33–36].

Electrochemical sensors are undergoing rapid development due to their unique and attractive advantages, including high sensitivity, rapid signal readout, low cost, and portability [37–39]. Dai et al. reported a CRISPR/Cas12a (cpf1) -based electrochemical biosensor (E-CRISPR) for the detection of human papillomavirus 16 (HPV-16) and parvovirus B19 (PB-19), which is more cost-effective and portable than biosensors based on optical-transduction [40]. Sheng et al. integrated the CRISPR/Cas13a system and a catalytic hairpin DNA circuit (CHDC) on a reusable electrochemical biosensor to detect non-small-cell lung carcinoma-related RNA [41]. Chaibun et al. reported an ultrasensitive electrochemical biosensor based on isothermal rolling circle amplification (RCA) for rapid detection of SARS-CoV-2 [42]. Ali et al. constructed a 3D nano-printed three-dimensional electrodes, coated with reduced-graphene-oxide and gold film combined with antigen and antibody for the detection of COVID-19 [43]. The electrochemical CRISPR/CHDC system is a fast, inexpensive and highly accurate tool for early cancer diagnosis.

To achieve the *trans*-cleavage of the ssDNA reporter through the CRISPR/Cas system on electrochemical sensors, ssDNA was fixed onto the working gold electrode through Au-SH bonds [44–46]. Although stable, gold electrodes or screen-printed gold electrodes are more expensive than carbon-glass electrodes or screen-printed carbon electrodes, and the formation of Au-SH bond takes as long as 12 h [47–52]. To solve this problem, we employed CeO_2 nanorods and poly (allylamine hydrochloride) (PAH) to randomly immobilize the ssDNA onto a screen-printed carbon electrode (SPCE). PAH is a positively-charged weak polyelectrolyte, and the positively charged PAH layer could attract negatively charged ssDNA through electrostatic adsorption [53,54]. The CeO_2 nanorods then immobilize ssDNA through the affinity of cerium to phosphate-containing ligands. The combination of PAH and CeO_2 enabled the facile immobilization of reporter ssDNA onto the electrode [55]. We demonstrated that ssDNA randomly distributed in the CeO_2/PAH complex on the electrode could be cleaved by activated Cas12a protein, and the ssDNA was fixed upright on the surface of the electrode. Based on this, we established a CRISPR ssDNA reporter immobilizing onto SPCE, dubbed CRISPR-SPCE, enabling the rapid diagnosis of COVID-19.

2. Materials and methods

2.1. Reagents and materials

The LbCas12a protein was expressed in *Escherichia coli* and purified as described previously [56]. The E gene fragment of SARS-CoV-2 (Wuhan-1 strain, GenBank: MN908947) was synthesized by GenScript (Nanjing, China) and was used as the target gene fragment template for the experiments [57]. A 228-bp fragment (Fig. 3) was amplified by PCR using the forward primer (PCR-F) and reverse primer (PCR-R). Reverse-transcription recombinase polymerase amplification was conducted using the GenDx ERA Kit (Suzhou GenDx Biotech, China). The RT-RPA for the E gene was performed using forward primer (RT-RPA-F) and reverse primer (RT-RPA-R). The crRNAs (Fig. 3) targeting E gene and ssDNA reporter (Fc-labeled ssDNA) were used for electrochemical detection. All oligonucleotides were synthesized by GenScript (Nanjing, China) and the detailed sequences are listed in Table S1. Pseudoviruses based on 4 coronavirus species, including SARS-CoV-2, hCov-HKU1, MERS-uPE and SARS-CoV-1 were purchased from Cobioer Biotechnology Company (Nanjing, China).

2.2. Synthesis of CeO_2 nanorods

CeO_2 nanorods were synthesized based on a previous report [58], with minor modifications as follows: 0.4 g of $CeCl_3{\cdot}7H_2O$ were dissolved in 15 mL ultrapure water, mixed with 20 mL of a 600 g L^{-1} NaOH solution and stirred for 30 min. Then, the mixture was transferred into a 50 mL high-pressure reaction vessel and kept at 140 °C for 24 h. After cooling the reaction vessel to room temperature, the product was washed with double distilled water until the pH became neutral and rinsed with ethanol several times. The resulting product was dried at 80 °C in an oven overnight.

2.3. Biosensor fabrication

The SPCE consisted of a silver pseudo-reference electrode, a carbon working electrode with a diameter of 3 mm, and a carbon counter electrode. To obtain a homogeneous dispersion, one mg of CeO_2 nanorods and 5 mg polyethyleneimine were dissolved in 1 mL water and sonicated for 5 min. Then, the CeO_2/PAH suspension and 2 μM ssDNA were mixed at equal proportion. The carbon working electrode was modified with 3 μL of the CeO_2/PAH/ssDNA mixture and left to dry at room temperature. The crRNA mixture (1 nM) contained crRNA1, crRNA2, crRNA3 and crRNA6 (0.25 nM, respectively, Fig. 3). The CRISPR/Cas12a reaction mix consisted of 2 μL 10 × Buffer, 1 μL CRISPR/Cas12a (200 ng μL^{-1}), 1 μL crRNA mixture (1 nM), 1 μL RNase Inhibitors (40 U μL^{-1}, Novoprotein, China), 1 μL the synthesized E gene fragment or RT-RPA product and nuclease-free water up to 20 μL. The buffer consisted of Tris-HCl (pH 7.5, 2 mM), glycerin (1%, v/v), and NaCl (0.5 mM). Then 20 μL of the CRISPR/Cas12a reaction mix was dropped on the surface of SPCE for *trans*-cleavage of ssDNA at 37 °C for 60 min.

2.4. Recombinase polymerase amplification

Isothermal amplification was conducted using the GenDx ERA Kit (Suzhou GenDx Biotech, China). Briefly, the RT-RPA was performed at 37 °C for 20 min in a 50 μL reaction comprising 25 μL of reaction buffer, 2.5 μL of RT-RPA-F (10 μM), 2.5 μL of RT-RPA-R (10 μM), 5 μL sample, 2.5 μL of magnesium acetate (280 mM), and ddH_2O to 50 μL. Reverse transcription of RNA was accomplished by the reverse transcriptase in the RT-RPA system at the same time. After amplification, 5 μL of the product was transferred to the Cas12a reaction system for electrochemical detection.

2.5. Electrochemical detection

Electrochemical measurements including cyclic voltammetry (CV) and differential pulse voltammetry (DPV) were performed in 100 mM Tris-HCl buffer pH 7.4. DPV with a potential range from −0.2 to 0.7 V, a scan rate of 0.05 V s^{-1}, an amplitude of 0.05 V and pulse width of 0.05 s was applied before and after the treatment with the CRISPR/Cas12a system to obtain the electrochemical signal change of ferrocene.

2.6. RT-qPCR assay

The RT-qPCR detection of the SARS-CoV-2 E gene was carried out according to the WHO recommended procedure [59]. The reaction system had a volume of 20 μL, consisting of 10 μL of 2 × Probe Master Mix (AceQ U+, Vazyme Biotech Co., Ltd., Nanjing, China), 0.4 μL of PCR-F, 0.4 μL of PCR-R, 0.2 μL of probe, 1 μL of template, and 8 μL of double distilled water. The reaction was carried at 37 °C for 2 min and 95 °C for 5 min, followed by 60 cycles at 95 °C for 10 s, and 60 °C for 30 s in a Bio-Rad CFX96 Touch RT-PCR system (Bio-Rad, USA). Reverse transcription of RNA was accomplished by the reverse transcriptase in the RT-PCR system.

3. Results and discussion

3.1. Working principle

The working principle of the biosensor is illustrated in Scheme 1. The RPA amplification reaction mixture containing primer and reverse transcriptase was used to convert amplified RNA from the samples into sufficient DNA. In the presence of the synthetic target gene fragment and crRNA, the Cas12a protein could be activated to exert its *trans*-cleavage activity on non-specific ssDNA. When the mixture containing the synthetic target gene fragment, Cas12a protein and crRNA was added onto the surface of SPCE modified with CeO_2/PAH/Fc-labeled ssDNA, the Fc-labeled ssDNA was cleaved by the activated Cas12a protein to induce a decrease of the electrochemical signals, which could be used for the detection of SARS-CoV-2.

3.2. Trans cleavage of CeO_2/PAH/Fc-labeled ssDNA on the surface SPCE by the CRISPR/Cas12a system

PAH binds DNA onto the SPCE through the electrostatic interactions between amine groups and the phosphate backbone [60]. Cerium is a heavy metal with a strong affinity to phosphate, which can also be used to adsorb DNA. As a result, PAH and CeO_2 nanorods were both used to immobilize Fc-labeled ssDNA onto SPCE.

Moreover, CeO_2 nanorods have excellent electrocatalytic properties, which also enhance the sensitivity [61]. The Ce^{3+} and Ce^{4+} oxidation states can easily gain and lose electrons to facilitate the electrochemical reaction. Finally, the oxygen vacancies in CeO_2 nanorods are also beneficial for improving oxygen mobility and enhancing the electrocatalysis ability [61].

Fig. 1A shows a TEM image of PAH-dispersed CeO_2 nanorods, indicating good dispersion. The length of the nanorods ranged from 150 to 220 nm, with an average value of approximately 200 nm. The XPS survey spectrum of the CeO_2 nanorods (Fig. 1B) identified the binding energies of C1s, Ce3d and O1s, indicating the chemical composition and valence states of CeO_2.

Cyclic voltammetry was used to investigate the performance of different SPCE. PAH/Fc-labeled ssDNA modified SPCE sensors (Fig. 2A, curve a). The curves showed a couple of weak redox peaks at 0.297 V and 0.247 V, indicating the successful immobilization of Fc-labeled ssDNA. In the presence of CeO_2 nanorods, the redox peaks became stronger, well defined and symmetric. These peaks occurred at 0.303 V and 0.273 V (ΔEp = 30 mV) indicating a higher electron transfer rate (Fig. 2A, curve b). CeO_2 nanorods combined with PAH were used to not only enhance the immobilization of ssDNA, but also accelerate electron transfer.

Then, we investigated the cleavage performance of the activated Cas12a-crRNA system on ssDNA immobilized on SPCE through DPV. The CeO_2/PAH/ssDNA modified SPCE showed a peak current value of 13.34 μA at 0.24 V (Fig. 2B curve a). After incubation with the Cas12a-crRNA system without the synthetic target gene fragment, the peak current practically did not exhibit any change at all (Fig. 2B, curve b), indicating that the Fc-labeled ssDNA was stably immobilized on the

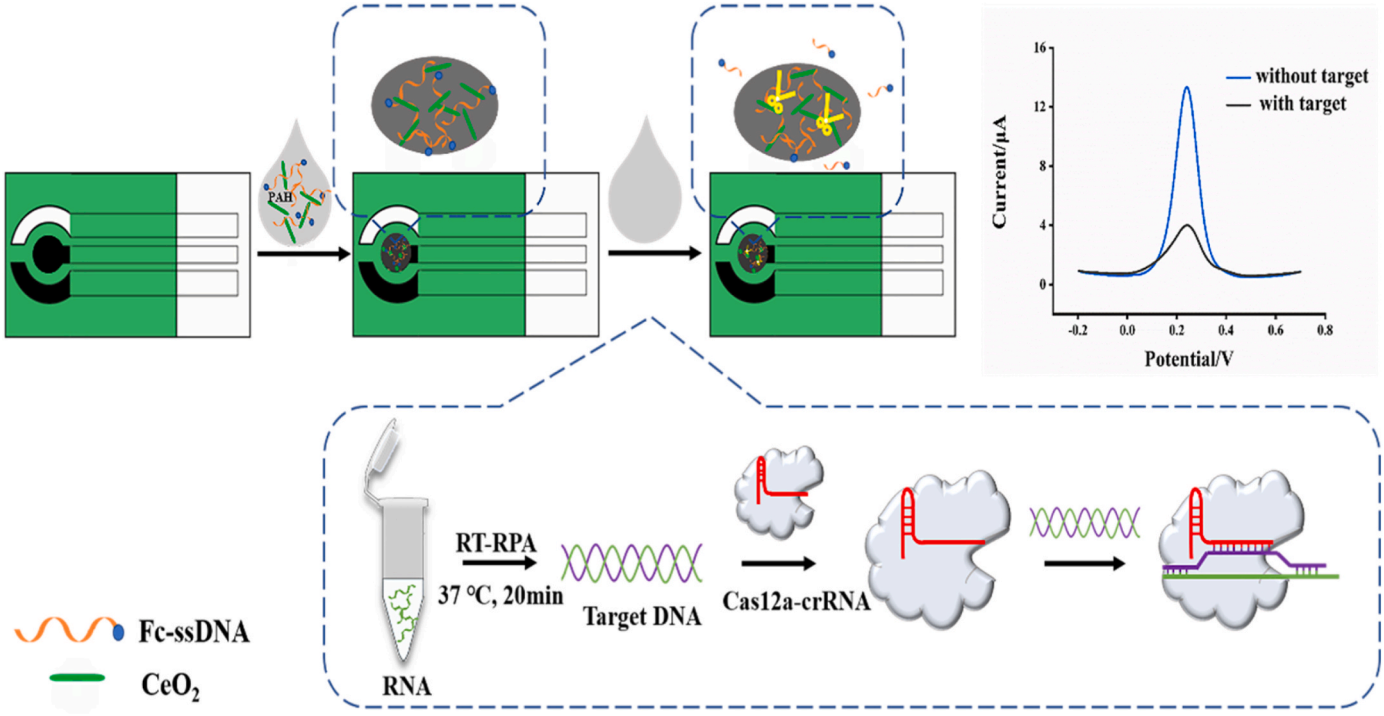

Scheme 1. Schematic illustration of the functional principle of CRISPR-SPCE.

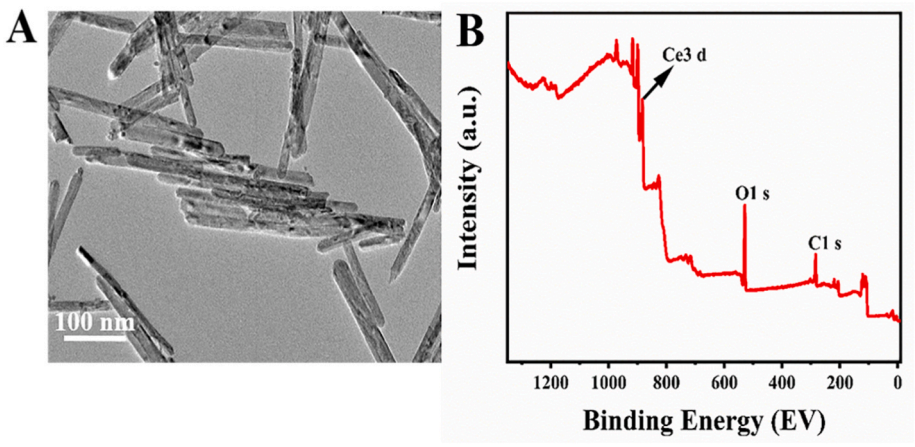

Fig. 1. (A) TEM image of PAH dispersed CeO_2 nanorods; (B) XPS survey spectrum of the CeO_2 nanorods.

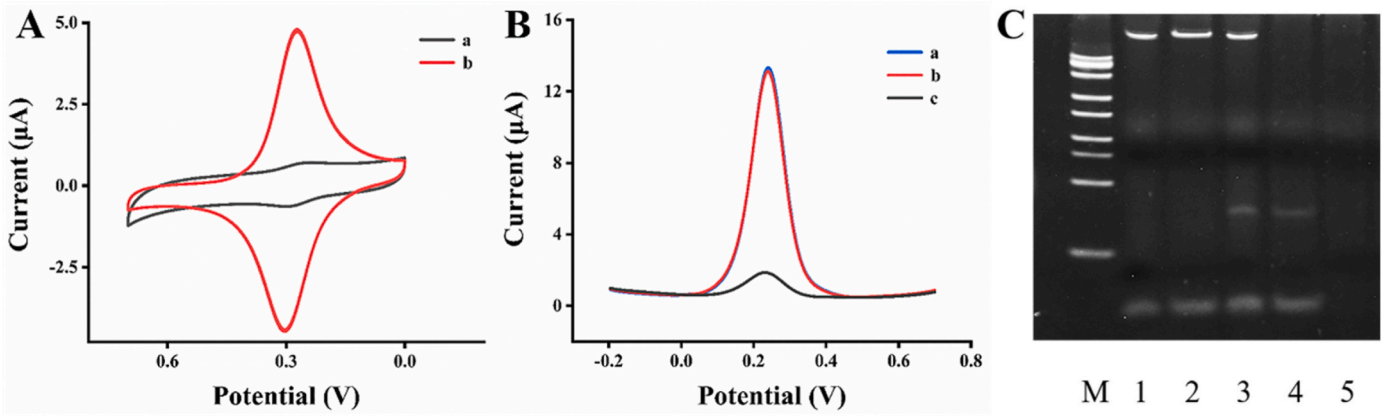

Fig. 2. (A) Cyclic voltammetry of PAH/Fc-labeled ssDNA modified SPCE biosensor (a) and CeO_2/PAH/Fc-labeled ssDNA modified SPCE (b); (B) DPV of modified SPCE before (a) and after incubation without target DNA (b), as well as after incubation with target DNA (c); (C) PAGE analysis of the ssDNA *trans*-cleavage ability of Cas12a. Lane 1: target DNA + Fc-labeled ssDNA; lane 2: Cas12a + target DNA + Fc-labeled ssDNA; lane 3: crRNA + target DNA + Fc-labeled ssDNA; lane 4: Cas12a + crRNA + Fc-labeled ssDNA; lane 5: Cas12a + crRNA + target DNA + Fc-labeled ssDNA.

electrode surface through CeO_2/PAH When the SPCE was incubated in the Cas12a-crRNA system with the synthetic target gene fragment for 60 min, the peak current significantly decreased from 13.34 to 1.869 μA due to the activated Cas12a protein cleaving the ssDNA on the SPCE surface, resulting in the Fc-labeled ssDNA fragment falling off. Taken together, the random DNA attached to the SPCE surface, as well as the ssDNA strands immobilized in an upright orientation on the electrode, could be cleaved by activated Cas12a protein, demonstrating the feasibility of the simple DNA immobilization method for the CRISPR/Cas system.

The *trans*-cleavage ability of CRISPR was also validated by polyacrylamide gel electrophoresis (Fig. 2C). The bands of the synthetic target gene fragment and Fc-labeled ssDNA complex are shown in lane 1. In the presence of Cas12a (lane 2), there was no change in the bands of the synthetic target gene fragment and ssDNA. In the presence of crRNA (lane 3), an additional upper band belonging to crRNA was observed. In the absence of the synthetic target gene fragment, the Cas12a/crRNA/ssDNA complex showed independent strips of crRNA and ssDNA, respectively (lane 4), indicating that Cas12a was inactive. In the presence of the synthetic target gene fragment, Cas12a was activated and indiscriminately cleaved ssDNA, leading to the disappearance of crRNA, synthetic target gene fragment and ssDNA (lane 5). These results indicated that *trans*-cleavage was only successful in the presence of Cas12a protein.

3.3. Optimization of reaction condition

The binding of crRNA to target sites could trigger the *trans*-cleavage of ssDNA. The CRISPR detection readout signal relies on the crRNA-dependent targeting cleavage efficiency, which is affected by the secondary structure and spacer sequence of the crRNA [62,63].

Six different crRNAs (crRNA1-crRNA6, Fig. 3) binding to different target sites were designed and evaluated under the optimized conditions for the detection of the synthetic target gene fragment (insert of Fig. 3). The "ΔI (%)"on the insert of Fig. 3 represents the percentage decrease of the ferrocene electrochemical signal before and after incubation with the activated CRISPR/Cas12a system. The six crRNAs showed obvious responses in the presence of the synthetic target gene fragment, indicating that all six crRNAs could bind to target sites and trigger the *trans*-cleavage of ssDNA. Furthermore, crRNA1-crRNA3 and crRNA6 showed more sensitive responses compared with crRNA4 and crRNA5. Thus, we chose the complex (1 nM) of crRNA1, crRNA3, crRNA3 and crRNA4 (0.25 nM respectively) for further experiments to obtain a strong detection signal, thus ensuring the stability of detection by avoiding the deactivation of crRNA recognition due to single nucleotide polymorphisms in the target region.

To achieve the best performance, experimental conditions such as the concentrations of CeO_2 and PAH as well as the incubation time of Fc-labeled ssDNA were investigated (Fig. 4A). The addition of CeO_2 nanorods increased the sensitivity of the electrochemical signal, while a

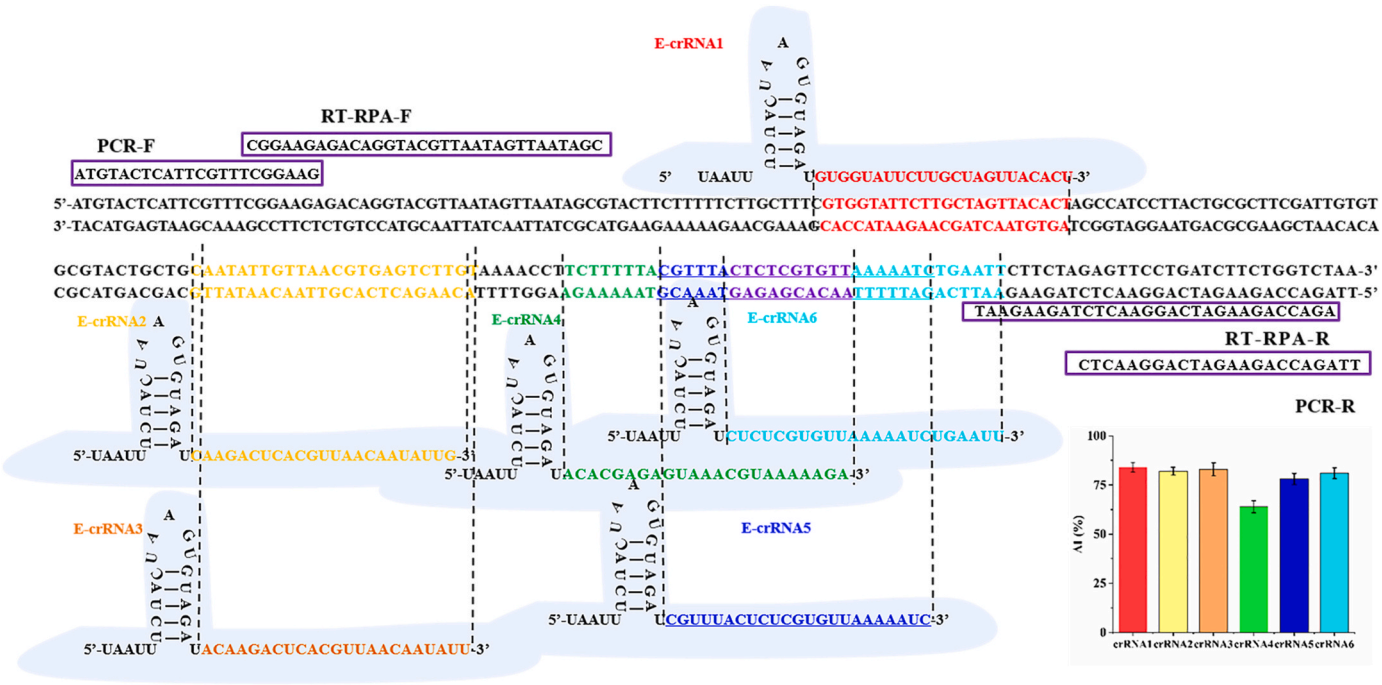

Fig. 3. Design of specific crRNAs targeting the E gene for SARS-CoV-2 detection.

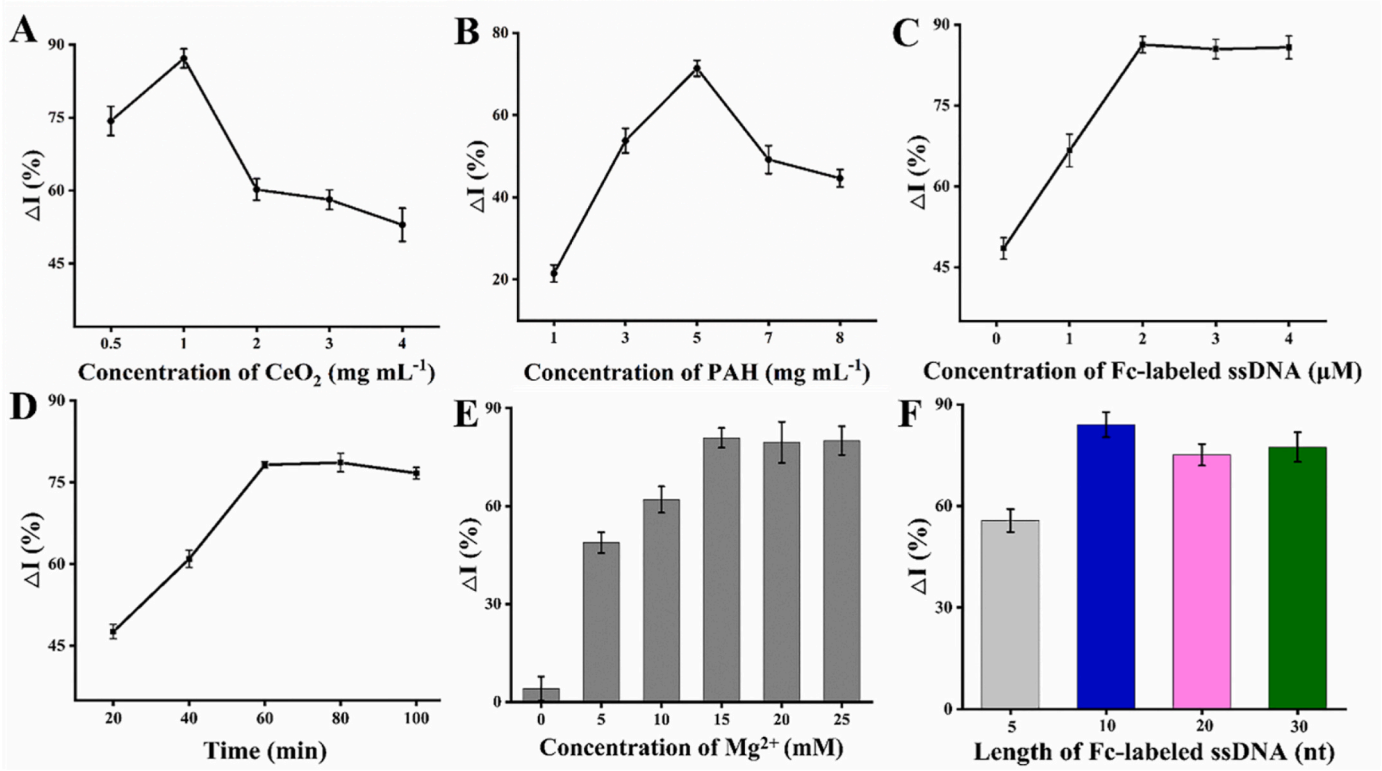

Fig. 4. Optimization of the detection conditions. Evaluation of the effects of (A) CeO_2 concentration; (B) PAH concentration; (C) Fc-labeled ssDNA concentration; (D) Incubation time and (E) Mg^{2+} concentration; (F) Comparison of signal change with Fc-labeled ssDNA of different lengths.

higher concentration might increase the background signal and decrease the ΔI (%), which was defined as the percentage decrease of ferrocene the electrochemical signal before and after incubation with the activated CRISPR/Cas12a system. Along with the increase of CeO_2 nanorod concentration from 0.5 to 4 mg mL^{-1}, the ΔI value reaches the maximal value at the concentration of 1 mg mL^{-1} and decreased in the range of 1.0–4.0 mg mL^{-1}. Therefore, 1.0 mg mL^{-1} was selected as the optimal concentration of CeO_2 nanorods.

Considering that the concentration of PAH would affect the amount of immobilized Fc-labeled ssDNA, ΔI gradually increased with the increasing of PAH concentration and reached its maximum value at 5.0 mg mL^{-1} (Fig. 4B). Accordingly, 5.0 mg mL^{-1} of PAH was selected for

sensitive detection.

It is well-known that the concentration of Fc-labeled ssDNA is also one of the critical factors affecting the sensitivity of the biosensor [64–66]. An excess of Fc-labeled ssDNA may result in shedding from the SPCE and impact the electrochemical signal. An appropriate concentration is beneficial to maintain stability and increase sensitivity. The results showed that 2 μmol L^{-1} Fc-labeled ssDNA resulted in maximal ΔI (Fig. 4C). The ΔI curve reached saturation in the range of 3.0–4.0 μmol L^{-1}, indicating that Fc-labeled ssDNA tended to be over-saturated. Thus, 2 μmol L^{-1} was chosen as the optimal concentration of Fc-labeled ssDNA.

In addition, the incubation time of SPCE in the CRISPR/Cas system which had a profound effect on the biosensor was optimized in the range from 10 min to 2 h. As depicted in Fig. 4D, the peak current increased from 20 min and tended to level off after 1 h, indicating the completion of *trans*-cleavage. Hence, 1 h was selected as the optimal incubation time for the CRISPR/Cas system with Fc-labeled ssDNA on SPCE.

Additionally, magnesium ions can promote the *trans*-cleavage process of the CRISPR/Cas12a system [67]. Consequently, the concentration of magnesium ions was also investigated, and 15 mM was selected as the optimal concentration (Fig. 4E). Also, the effect of the length of the Fc-labeled ssDNA fragments on the *trans*-cleavage activity was investigated (Fig. 4F). Fc-labeled ssDNA with a length of 5 nt had a lower response, probably due to the distance hindering the *trans*-cleavage of Cas12a, while lengths from 10 to 30 nt had comparable results. Therefore, an ssDNA length of 10 nt was selected for this system.

3.4. Sensitivity, detection limit and stability

The sensitivity of the system was investigated under the optimized conditions. With increasing amounts of the E gene fragment of SARS-CoV-2, the peak current of ferrocene decreased and ΔI increased (Fig. 5A). The current response showed a linear relationship with the amount of the synthetic target gene fragment in the concentration range of 2×10^{-8} to 5×10^{-5} ng μL^{-1} and the detection limit was calculated to be 5.0×10^{-9} ng μL^{-1}.

By utilizing RPA, the sensitivity of the CRISPR/Cas system was enhanced more than 100-fold, resulting in a limit of detection (LOD) of 5.0×10^{-11} ng μL^{-1} (0.27 copies μL^{-1}). The comparison shown in results Table 1 indicates that the proposed method has higher sensitivity than previously reported methods [68–76].

The increased sensitivity was a result of the electrochemical method and the immobilization method. Electrochemical methods are generally recognized as highly sensitive. Fc-labeled ssDNA was immobilized on the electrode through PAH and CeO_2 nanorods. The electrostatic interactions of PAH [53,54] and the adsorption affinity of CeO_2 [55] resulted in the immobilization of large amounts of ssDNA, which improved the sensitivity.

Table 1
Comparison with reported methods for SARS-CoV-2 detection.

Assays	Target	Limit of detection	Refs.
DNA nanoscaffold-based hybrid chain reaction colorimetric assay	SARS-CoV-2 RNA	0.96 pM (5.78×10^5 copies μL^{-1})	[68]
CRISPR-Cas12a fluorescence detection	N gene	3 copies μL^{-1}	[69]
CRISPR-Cas12a Lateral flow visual detection	ORF1ab and N genes	7 copies μL^{-1}	[70]
CRISPR-Cas12a Lateral flow visual detection	E and N genes	10 copies μL^{-1}	[71]
CRISPR-Cas13a SHERLOCK	S, N and Orf1ab genes	42 copies $reaction^{-1}$ (2.1 copies μL^{-1})	[72]
CRISPR-Cas12a LAMP Lateral flow visual detection	N gene	2 copies μL^{-1}	[73]
Paper based electrochemical	SARS-CoV-2 RNA	6.9 copies μL^{-1}	[74]
CRISPR/Cas13a electrochemical biosensor	ORF and S genes	0.14 copies μL^{-1} and 0.75 copies μL^{-1}	[75]
4WJ-based electrochemical biosensor	S gene and Orf1ab gene	2 copies μL^{-1} and 3 copies μL^{-1}	[76]
CRISPR-SPCE	E gene	0.27 copies μL^{-1}	This work

To investigate the stability of the proposed biosensor, the fabricated biosensor was stored at room temperature and used for measurements after 7 and 10 days, respectively. The biosensor retained 99.35% and 98.67% of the initial electrochemical signal after 7 days and 10 days, respectively. These results demonstrated that Fc-labeled ssDNA was stably conjugated onto the surface of SPCE, and remained functional for the detection of SARS-CoV-2 after prolonged storage.

3.5. Specificity and application in sample analysis

To assess the specificity of the SPCE sensors, pseudovirus corresponding to hCov-HKU1-E, MERS-uPE/E and SARS-CoV-1 were used as interfering analytes. The concentration of interfering pseudovirus was 10 times higher than that of SARS-CoV-2. As shown in Fig. 6, no significant changes were found after the addition of interfering pseudoviruses, indicating excellent specificity.

We also applied the CRISPR/Cas system to detect SARS-CoV-2 in different samples. Human throat swabs, frozen food and frozen food packaging materials were collected to validate the practical applicability of the sensor. Throat swab samples were collected from volunteers,

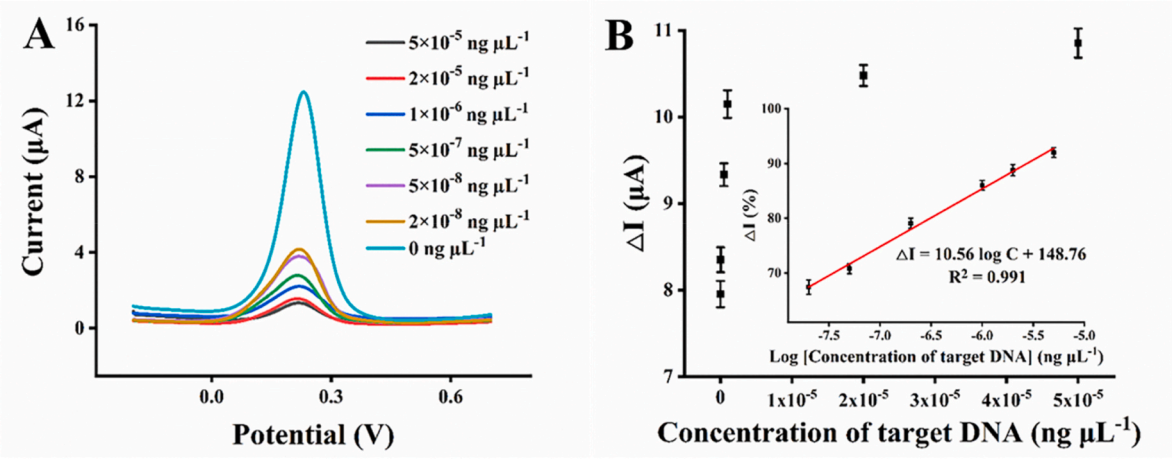

Fig. 5. (A) DPV with different concentrations of target DNA; (B) The linear calibration curve in the range of 2.0×10^{-8} to 5.0×10^{-5} ng μL^{-1}.

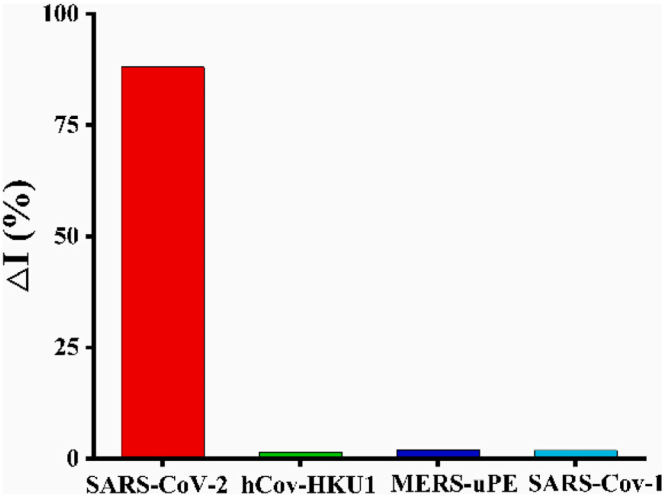

Fig. 6. The selectivity of the proposed system in the detection of SARS-CoV-2.

while frozen food and frozen food packaging were purchased from Yonghui supermarket. The samples were preprocessed according to the standard TCAQI159-2020 "Sampling and real-time RT-PCR assay for detection of SARS-CoV-2 in food and food packaging surfaces". Insert the swab into the sampling tube with 3.0 mL sampling solution and 1.0 mL 0, 10, 20, 200 copies μL^{-1} of SARS-CoV-2 pseudoviruses, respectively. Different concentrations of each ingredient were used to verify the detection ability of the system at different concentration levels. The spiked samples were prepared and used to extract genomic RNA, which was reverse-transcribed and used as template. RT-qPCR and the CRISPR-SPCE system were used to test the samples in parallel to verify the consistency of the two methods. The RT-qPCR method is a standard method commonly used in clinical practice. As shown in Table S2, a total of 50 samples were used in qPCR and CRISPR-SPCE tests, including 26 human throat swab samples, 16 frozen shrimp samples, and 8 frozen food packaging materials samples. Among the 50 samples, 37 samples were determined to be positive and 13 samples were negative by both qPCR and CRISPR-SPCE methods. And the results of the two methods qPCR and CRISPR-SPCE were 100% consistent, demonstrating that the great potential of the CRISPR-SPCE system in quantifying SARS-CoV-2 in real samples. The CRISPR-SPCE sensor offers a cost-effective strategy for the quantification of disease biomarkers.

4. Conclusions

In this study, we successfully demonstrated that ssDNA randomly immobilized on the electrode, as well as upright immobilized ssDNA could be cleaved by the CRISPR/Cas system. This result demonstrated the feasibility of applying a carbon-based electrode instead of a gold-based electrode for CRISPR/Cas detection, which could reduce the cost and shorten the detection time. CeO_2 nanorods and PAH were used for random immobilization of the ssDNA on SPCE. Finally, CRISPR-SPCE was successfully used for the detection of SARS-CoV-2 pseudoviruses. The proposed method only requires minimal equipment, indicating its great potential for point-of-care diagnosis. The detection of SARS-CoV-2 in throat swabs, frozen food, and frozen food packaging materials demonstrates the feasibility of using this system in clinical diagnosis and frozen food monitoring.

CRediT authorship contribution statement

Lina Wu: Data curation, Writing – original draft. **Xinjie Wang:** Writing – review & editing, Supervision. **Chengyuan Wu:** Data Collection, Data curation, Formal analysis. **Xizhong Cao:** Methodology, Data curation. **Taishan Tang:** Writing – review & editing. **He Huang:** Conceptualization, Supervision. **Xingxu Huang:** Conceptualization, Supervision, Funding acquisition.

Declaration of competing interest

The authors declare that they have no known competing financial interests or personal relationships that could have appeared to influence the work reported in this paper.

Acknowledgments

This study was sponsored by the Key Research Project of Zhejiang Laboratory, the emergency key program of Guangzhou Laboratory (EKPG21-18), and a Shanghai local grant (21N31900400).

Appendix A. Supplementary data

Supplementary data to this article can be found online at https://doi.org/10.1016/j.aca.2022.340120.

References

[1] Y.X. Wang, Y. Zhang, J.B. Chen, M.J. Wang, T. Zhang, W.X. Luo, Y.L. Li, Y.P. Wu, B. Zeng, K.X. Zhang, R.J. Deng, W.M. Li, Detection of SARS-CoV-2 and its mutated variants via CRISPR-cas13-based transcription amplification, Anal. Chem. 93 (7) (2021) 3393–3402.
[2] K.F. Yang, J.C. Chaput, REVEALR: a multicomponent XNAzyme-based nucleic acid detection system for SARS-CoV-2, J. Am. Chem. Soc. 143 (24) (2021) 8957–8961.
[3] B.J. Shan, Y.Y. Broza, W.J. Li, Y. Wang, S.H. Wu, Z.Z. Liu, J. Wang, S.Y. Gui, L. Wang, Z.H. Zhang, W. Liu, S.B. Zhou, W. Jin, Q.Y. Zhang, D.D. Hu, L. Lin, Q. J. Zhang, W. Li, J.Q. Wang, H. Liu, Y.Y. Pan, H. Haick, Multiplexed nanomaterial-based sensor array for detection of COVID-19 in exhaled breath, ACS Nano 14 (9) (2020) 12125–12132.
[4] P. Fozouni, S.M. Son, M.D.D. Derby, G.J. Knott, C.N. Gray, M.V. D'Ambrosio, C. Y. Zhao, N.A. Switz, G.R. Kumar, S.I. Stephens, D. Boehm, C.-L. Tsou, J. Shu, A. Bhuiya, M. Armstrong, A.R. Harris, P.-Y. Chen, J.M. Osterloh, A. Meyer-Franke, B. Joehnk, K. Walcott, A. Sil, C. Langelier, K.S. Pollard, E.D. Crawford, A. S. Puschnik, M. Phelps, A. Kistler, J.L. DeRisi, J.A. Doudna, D.A. Fletcher, M. Ott, Amplification-free detection of SARS-CoV-2 with CRISPR-Cas13a and mobile phone microscopy, Cell 184 (2) (2021) 323–333.
[5] L.V. Maria, E.N. Carmen, R.D. Ciro, P. Demian, C. Milagros, M.R. Paula, M. G. Carlos, C. Rocio, A. Melanie, C. Rafael, G. Juan Carlos, M. Rodolfo, S. Alvaro, S. Begona, CASCADE: naked eye-detection of SARS-CoV-2 using Cas13a and gold nanoparticles, Anal. Chim. Acta 1205 (2022), 339749.
[6] H.W. Zhou, D.L. Liu, L. Ma, T.T. Ma, T.Y. Xu, L.L. Ren, L. Li, S.H. Xu, A SARS-CoV-2 reference standard quantified by multiple digital PCR platforms for quality assessment of molecular tests, Anal. Chem. 93 (2) (2021) 715–721.
[7] Z.Q. Yao, Q.D. Zhang, W.T. Zhu, M. Galluzzi, W.H. Zhou, J. Li, A.V. Zayats, X.-F. Yu, Rapid detection of SARS-CoV-2 viral nucleic acids based on surface enhanced infrared absorption spectroscopy, Nanoscale 13 (22) (2021) 10133–10142.
[8] H. Chen, S.K. Park, Y.J. Joung, T. Kang, M.K. Lee, J. Choo, SERS-based dual-mode DNA aptasensors for rapid classification of SARS-CoV-2 and influenza A/H1N1 infection, Sens. Actuators B Chem. 355 (2022), 131324.
[9] T. Beduk, D. Beduk, J.I. de Oliveira, F. Zihnioglu, C. Cicek, R. Sertoz, B. Arda, T. Goksel, K. Turhan, K.N. Salama, S. Timu, Rapid point-of-care COVID-19 diagnosis with a gold-nanoarchitecture-assisted laser-scribed graphene biosensor, Anal. Chem. 93 (24) (2021) 8585–8594.
[10] B. Yao, J. Zhang, Z.Q. Fan, Y.D. Ding, B. Zhou, R.L. Yang, J.F. Zhao, K. Zhang, Rational engineering of the DNA walker amplification strategy by using a Au@Ti_3C_2@PEI-Ru(dcbpy)$_3^{2+}$ nanocomposite biosensor for detection of the SARS-CoV-2 RdRp gene, ACS Appl. Mater. Interfaces 13 (17) (2021) 19816–19824.
[11] G.H. Xun, S.T. Lane, V.A. Petrov, B.E. Pepa, H.M. Zhao, A rapid, accurate, scalable, and portable testing system for COVID-19 diagnosis, Nat. Commun. 12 (1) (2021) 2905.
[12] J.S. Park, K. Hsieh, L.B. Chen, A. Kaushik, A.Y. Trick, T.-H. Wang, Digital CRISPR/Cas-Assisted assay for rapid and sensitive detection of SARS-CoV-2, Adv. Sci. 8 (5) (2021), 2003564.
[13] P.X. Ma, Q.Z. Meng, B.Q. Sun, B. Zhao, L. Dang, M.T. Zhong, S.Y. Liu, H.T. Xu, H. Mei, J. Liu, T. Chi, G. Yang, M. Liu, X.X. Huang, X.J. Wang, MeCas12a, a highly sensitive and specific system for COVID-19 detection, Adv. Sci. 7 (20) (2020), 2001300.
[14] K. Zhang, Z.Q. Fan, B. Yao, Y.D. Ding, J. Zhao, M.H. Xie, J.B. Pan, Exploring the trans-cleavage activity of CRISPR-Cas12a for the development of a Mxene based electrochemiluminescence biosensor for the detection of Siglec-5, Biosens, Bioelectron 178 (2021), 113019.
[15] T. Zhou, M.Q. Huang, J.Q. Lin, R. Huang, D. Xing, High-fidelity CRISPR/Cas13a trans-cleavage-triggered rolling circle amplified DNAzyme for visual profiling of MicroRNA, Anal. Chem. 93 (4) (2021) 2038–2044.

[16] S. Svitashev, C. Schwartz, B. Lenderts, J.K. Young, A.M. Cigan, Genome editing in maize directed by CRISPR-Cas9 ribonucleoprotein complexes, Nat. Commun. 7 (2016), 13274.

[17] Y. Lee, J. Choi, H.K. Han, S. Park, S.Y. Park, C. Park, C. Baek, T. Lee, J. Min, Fabrication of ultrasensitive electrochemical biosensor for dengue fever viral RNA Based on CRISPR/Cpf1 reaction, Sens. Actuators B Chem. 326 (2021), 128677.

[18] S.C. Knight, R. Tjian, J.A. Doudna, Genome im Fokus: entwicklung und Anwendungen von CRISPR-Cas9-Bildgebungstechnologien, Angew. Chem. 130 (16) (2018) 4412–4420.

[19] C.H. Gabriel, M. del Olmo, A. Zehtabian, M. Jäger, S. Reischl, H. van Dijk, C. Ulbricht, A. Rakhymzhan, T. Korte, B. Koller, A. Grudziecki, B. Maier, A. Herrmann, R. Niesner, T. Zemojtel, H. Ewers, A.E. Granada, H. Herzel, A. Kramer, Live-cell imaging of circadian clock protein dynamics in CRISPR-generated knock-in cells, Nat. Commun. 12 (1) (2021) 3796.

[20] B.H. Chen, W. Zou, H.Y. Xu, Y. Liang, B. Huang, Efficient labeling and imaging of protein-coding genes in living cells using CRISPR-Tag, Nat. Commun. 9 (2018) 5065.

[21] L.-Z. Yang, Y. Wang, S.-Q. Li, R.-W. Yao, P.-F. Luan, H. Wu, G.G. Carmichael, L.-L. Chen, Dynamic imaging of RNA in living cells by CRISPR-cas13 systems, Mol. Cell 76 (6) (2019) 981–997.

[22] T. Wan, Y. Ping, Delivery of genome-editing biomacromolecules for treatment of lung genetic disorders, Adv. Drug Deliv. Rev. 168 (2021) 196–216.

[23] K. Musunuru, A.C. Chadwick, T. Mizoguchi, S.P. Garcia, J.E. DeNizio, C.W. Reiss, K. Wang, S. Iyer, C. Dutta, V. Clendaniel, M. Amaonye, A. Beach, K. Berth, S. Biswas, M.C. Braun, H.-M. Chen, T.V. Colace, J.D. Ganey, S.A. Gangopadhyay, R. Garrity, L.N. Kasiewicz, J. Lavoie, J.A. Madsen, Y. Matsumoto, A.M. Mazzola, Y. S. Nasrullah, J. Nneji, H. Ren, A. Sanjeev, M. Shay, M.R. Stahley, S.H.Y. Fan, Y. K. Tam, N.M. Gaudelli, G. Ciaramella, L.E. Stolz, P. Malyala, C.J. Cheng, K. G. Rajeev, E. Rohde, A.M. Bellinger, S. Kathiresan, In vivo CRISPR base editing of PCSK9 durably lowers cholesterol in primates, Nature 593 (7859) (2021) 429–434.

[24] M. Martinez-Lage, R. Torres-Ruiz, P. Puig-Serra, P. Moreno-Gaona, M.C. Martin, F. J. Moya, O. Quintana-Bustamante, S. Garcia-Silva, A.M. Carcaboso, P. Petazzi, C. Bueno, J. Mora, H. Peinado, J.C. Segovia, P. Menendez, S. Rodriguez-Perales, In vivo CRISPR/Cas9 targeting of fusion oncogenes for selective elimination of cancer cells, Nat. Commun. 11 (1) (2020) 5060.

[25] S.Y. Xie, Z.R. Ji, T.Y. Suo, B.Z. Li, X. Zhang, Advancing sensing technology with CRISPR: from the detection of nucleic acids to a broad range of analytese-A review, Anal. Chim. Acta 1185 (2021), 338848.

[26] J.J. Shen, X.M. Zhou, Y.Y. Shan, H.H. Yue, R. Huang, J.M. Hu, D. Xing, Sensitive detection of a bacterial pathogen using allosteric probe-initiated catalysis and CRISPR-Cas13a amplification reaction, Nat. Commun. 11 (1) (2020) 267.

[27] H. Wu, X.Y. Chen, M.Y. Zhang, X.F. Wang, Y.J. Chen, C. Qian, J. Wu, J.F. Xu, Versatile detection with CRISPR/Cas system from applications to challenges, Trends Anal. Chem. 135 (2021), 116150.

[28] R. Nouri, Z.F. Tang, M. Dong, T.Y. Liu, A. Kshirsagar, W.H. Guan, CRISPR-based detection of SARS-CoV-2: a review from sample to result, Biosens. Bioelectron. 178 (2021), 113012.

[29] K. Shi, S.Y. Xie, R.Y. Tian, S. Wang, Q. Lu, D.H. Gao, C.Y. Lei, H.Z. Zhu, Z. Nie, A CRISPR-Cas autocatalysis-driven feedback amplification network for supersensitive DNA diagnostics, Sci. Adv. 7 (5) (2021), eabc7802.

[30] Y. Li, S.Y. Li, J. Wang, G. Liu, CRISPR/Cas systems towards next-generation biosensing, Trends Biotechnol 37 (7) (2019) 730–743.

[31] J.-H. Choi, J. Lim, M. Shin, S.-H. Paek, J.-W. Choi, CRISPR-Cas12a-Based nucleic acid amplification-free DNA biosensor via Au nanoparticle-assisted metal-enhanced fluorescence and colorimetric analysis, Nano Lett 21 (1) (2021) 693–699.

[32] H. Wu, Y.J. Chen, Y. Shi, L. Wang, M.Y. Zhang, J. Wu, H. Chen, Carrying out pseudo dual nucleic acid detection from sample to visual result in a polypropylene bag with CRISPR/Cas12a, Biosens. Bioelectron. 178 (2021), 113001.

[33] J.S. Gootenberg, O.O. Abdauueh, J.W. Lee, P. Essletzbichler, A.J. Dy, J. Joung, V. Verdine, N. Donghia, N.M. Daringer, C.A. Frejie, C. Myhrvold, R. P. Bhattacharyya, J. Livny, A. Regev, E.V. Koonin, D.T. Hung, P.C. Sabeti, J. J. Collions, F. Zhang, Nucleic acid detection with CRISPR-Cas13a/C2c2, Science 356 (6336) (2017) 438–442.

[34] J.S. Gootenberg, O.O. Abudayyeh, M.J. Kellner, J. Joung, J.J. Collins, F. Zhang, Multiplexed and portable nucleic acid detection platform with Cas13, Cas12a, and Csm6, Science 360 (6387) (2018) 439–444.

[35] C. Myhrvold, C.A. Freije, J.S. Gootenberg, O.O. Abudayyeh, H.C. Metsky, A. F. Durbin, M.J. Kellner, A.L. Tan, L.M. Paul, L.A. Parham, K.F. Garcia, K.G. Barnes, B. Chak, A. Mondini, M.L. Nogueira, S. Isern, S.F. Michael, I. Lorenzana, N. L. Yozwiak, B.L. MacInnis, I. Bosch, L. Gehrke, F. Zhang, P.C. Sabeti, Field-deployable viral diagnostics using CRISPR-Cas13, Science 360 (6387) (2018) 444–448.

[36] J.S. Chen, E.B. Ma, L.B. Harrington, M. Da Costa, X.R. Tian, J.M. Palefsky, J. A. Doudna, CRISPR-Cas12a target binding unleashes indiscriminate single-stranded DNase activity, Science 360 (6387) (2018) 436–439.

[37] X.X. Zhao, S.S. Li, G. Liu, Z. Wang, Z.H. Yang, Q.W. Zhang, M.D. Liang, J.K. Liu, Z. L. Li, Y.J. Tong, G.L. Zhu, X.Y. Wang, L. Jiang, W.S. Wang, G.-Y. Tan, L.X. Zhang, A versatile biosensing platform coupling CRISPR–Cas12a and aptamers for detection of diverse analytes, Sci. Bull. 66 (1) (2021) 69–77.

[38] F. Li, Q.H. Ye, M.T. Chen, B.Q. Zhou, J.M. Zhang, R. Pang, L. Xue, J. Wang, H. Y. Zeng, S. Wu, Y.X. Zhang, Y. Ding, Q.P. Wu, An ultrasensitive CRISPR/Cas12a based electrochemical biosensor for Listeria monocytogenes detection, Biosens. Bioelectron. 179 (2021), 113073.

[39] S.D. Bukkitgar, N.P. Shetti, T.M. Aminabhavi, Electrochemical investigations for COVID-19 detection-A comparison with other viral detection methods, Chem. Eng. J. 420 (2) (2021), 127575.

[40] Y.F. Dai, R.A. Somoza, L. Wang, J.F. Welter, Y. Li, A.I. Caplan, C.C. Liu, Exploring the trans-cleavage activity of CRISPR-cas12a (cpf1) for the development of a universal electrochemical biosensor, Angew. Chem. Int. Ed. 58 (48) (2019) 17399–17405.

[41] Y. Sheng, T.H. Zhang, S.H. Zhang, M. Johnston, X.H. Zheng, Y.Y. Shan, T. Liu, Z. N. Huang, F.Y. Qian, Z.H. Xie, Y.R. Ai, H.K. Zhong, T.R. Kuang, C. Dincer, G. A. Urbane, J.M. Hu, A CRISPR/Cas13a-powered catalytic electrochemical biosensor for successive and highly sensitive RNA diagnostics, Biosens. Bioelectron. 178 (2021), 113027.

[42] T. Chaibun, J. Puenpa, T. Ngamdee, N. Boonapatcharoen, P. Athamanolap, A. P. O'Mullane, S. Vongpunsawad, Y. Poovorawan, S.Y. Lee, B. Lertanantawong, Rapid electrochemical detection of coronavirus SARS-CoV-2, Nat. Commun. 12 (1) (2021) 802.

[43] M.A. Ali, C.S. Hu, S. Jahan, B. Yuan, M.S. Saleh, E.G. Ju, S.-J. Gao, R. Panat, Sensing of COVID-19 antibodies in seconds via aerosol jet nanoprinted reduced-graphene-oxide-coated 3D electrodes, Adv. Mater. 33 (7) (2021), 2006647.

[44] P.-F. Liu, K.-R. Zhao, Z.-J. Liu, L. Wang, S.-Y. Ye, G.-X. Liang, Cas12a-based electrochemiluminescence biosensor for target amplification-free DNA detection, Biosens. Bioelectron. 176 (2021), 112954.

[45] Y. Cui, S.J. Fane, Z. Yuan, M.H. Song, J.W. Hu, D. Qian, D.S. Zhen, J.H. Li, B. D. Zhu, Ultrasensitive electrochemical assay for microRNA-21 based on CRISPR/Cas13a-assisted catalytic hairpin assembly, Talanta 224 (2021), 121878.

[46] D.C. Zhang, Y.R. Yan, H.Y. Que, T.T. Yang, X.X. Cheng, S.J. Ding, X.M. Zhang, W. Cheng, CRISPR/Cas12a-Mediated interfacial cleaving of hairpin DNA reporter for electrochemical nucleic acid sensing, ACS Sens 5 (2) (2020) 557–562.

[47] K.-R. Zhao, L. Wang, P.-F. Liu, X.-M. Hang, H.-Y. Wang, S.-Y. Ye, Z.-J. Liu, G.-X. Liang, A signal-switchable electrochemiluminescence biosensor based on the integration of spherical nucleic acid and CRISPR/Cas12a for multiplex detection of HIV/HPV DNAs, Sens. Actuators B Chem. 346 (2021), 130485.

[48] H.H. Chen, Y.H. Xiang, R.F. Cai, L. Zhang, Y.T. Zhang, N.D. Zhou, An ultrasensitive biosensor for dual-specific DNA based on deposition of polyaniline on a self-assembled multi-functional DNA hexahedral-nanostructure, Biosens. Bioelectron. 179 (2021), 113066.

[49] K. Zhang, W.T. Huang, H. Li, M.H. Xie, J.Y. Wang, Ultrasensitive detection of hERG potassium channel in single-cell with photocleavable and entropy-driven reactions by using an electrochemical biosensor, Biosens. Bioelectron. 132 (2019) 310–318.

[50] K. Zhang, Z.Q. Fan, B. Yao, T.T. Zhang, Y.D. Ding, S. Zhu, M.H. Xie, Entropy-driven electrochemiluminescence ultra-sensitive detection strategy of NF-κB p50 as the regulator of cytokine storm, Biosens. Bioelectron. 176 (2021), 112942.

[51] D.D. Li, Y.X. Xu, L. Fan, B. Shen, X.J. Ding, R. Yuan, X.M. Li, W.X. Chen, Target-driven rolling walker based electrochemical biosensor for ultrasensitive detection of circulating tumor DNA using doxorubicin@tetrahedron-Au tags, Biosens. Bioelectron. 148 (2020), 111826.

[52] X.Q. Zhang, Y. Feng, S.Y. Duan, L.L. Su, J.L. Zhang, F.J. He, Mycobacterium tuberculosis strain H37Rv electrochemical sensor mediated by aptamer and AuNPs-DNA, ACS Sens 4 (4) (2019) 849–855.

[53] T.S. Bronder, A. Poghossian, M.P. Jessing, M. Keusgen, M.J. Schöning, Surface regeneration and reusability of label-free DNA biosensors based on weak polyelectrolyte-modified capacitive field-effect structures, Biosens. Bioelectron. 126 (2019) 510–517.

[54] S. Roy, A. Jaiswal, DNA binding and NIR triggered DNA release from quaternary ammonium modified poly(allylamine hydrochloride) functionalized and folic acid conjugated reduced graphene oxide nanocomposites, Int. J. Biol. Macromol. 153 (2020) 931–941.

[55] B.W. Liu, Z.Y. Sun, P.-J.J. Huang, J.W. Liu, Hydrogen peroxide displacing DNA from nanoceria: mechanism and detection of glucose in serum, J. Am. Chem. Soc. 137 (3) (2015) 1290–1295.

[56] X.J. Wang, P.P. Ji, H.Y. Fan, L. Dang, W.W. Wan, S.Y. Liu, Y.H. Li, W.X. Yu, X.Y. Li, X.D. Ma, X. Ma, Q. Zhao, X.X. Huang, M. Liao, CRISPR/Cas12a technology combined with immunochromatographic strips for portable detection of African swine fever virus, Commun. Biol. 3 (1) (2020) 62.

[57] X.J. Wang, M.T. Zhong, Y. Liu, P.X. Ma, L. Dang, Q.Z. Meng, W.W. Wan, X.D. Ma, J. Liu, G. Yang, Z.F. Yang, X.X. Huang, M. Liu, Rapid and sensitive detection of COVID-19 using CRISPR/Cas12a-based detection with naked eye readout, CRISPR/Cas12a-NER, Sci. Bull. 65 (17) (2020) 1436–1439.

[58] Q. Wu, F. Zhang, P. Xiao, H.S. Tao, X.Z. Wang, Z. Hu, Great influence of anions for controllable synthesis of CeO_2 nanostructures: from nanorods to nanocubes, J. Phys. Chem. C 112 (44) (2008) 17076–17080.

[59] World Health Organization, Laboratory Testing for 2019 Novel Coronavirus (2019-nCoV) in Suspected Human Cases, 2020. https://www.who.int/publications/i/item/10665-331501.

[60] H.Y. Liu, J.W. Liu, Self-limited phosphatase-mimicking CeO_2 nanozymes, ChemNanoMat 6 (6) (2020) 947–952.

[61] J.D. Wang, X. Xiao, Y. Liu, K.M. Pan, H. Pang, S.Z. Wei, The application of CeO_2-based materials in electrocatalysis, J. Mater. Chem. A 7 (30) (2019) 17675–17702.

[62] S. Creutzburg, W.Y. Wu, P. Mohanraju, T. Swartjes, F. Alkan, J. Gorodkin, R.H. J. Staals, J. van der Oost, Good guide, bad guide: spacer sequence-dependent cleavage efficiency of Cas12a, Nucleic Acids Res 48 (6) (2020) 3228–3243.

[63] H.K. Kim, M. Song, J. Lee, A.V. Menon, S. Jung, Y.M. Kang, J.W. Choi, E. Woo, H. C. Koh, J.W. Nam, H. Kim, In vivo high-throughput profiling of crispr-cpf1 activity, Nat. Methods 14 (2) (2017) 153–159.

[64] Y.L. Ji, J.X. Guo, B.X. Ye, G.H. Peng, C. Zhang, L.N. Zou, An ultrasensitive carcinoembryonic antigen electrochemical aptasensor based on 3D DNA nanoprobe and Exo III, Biosens. Bioelectron. 196 (2022), 113741.
[65] H.Q. Yang, Y. Xu, Q.Q. Hou, Q.Z. Xu, C.F. Ding, Magnetic antifouling material based ratiometric electrochemical biosensor for the accurate detection of CEA in clinical serum, Biosens. Bioelectron. 208 (2022), 114216.
[66] Z.J. Qiao, Y.C. Yan, S. Bi, Three-dimensional DNA structures in situ decorated with metal nanoclusters for dual-mode biosensing of glucose, Sens. Actuators B Chem 352 (2) (2022), 131073.
[67] D. Dong, K. Ren, X.L. Qiu, J.L. Zheng, M.H. Guo, X.Y. Guan, H.N. Liu, N.N. Li, B. L. Zhang, D.J. Yang, C. Ma, S. Wang, D. Wu, Y.F. Ma, S.L. Fan, J.W. Wang, N. Gao, Z.W. Huang, The crystal structure of Cpf1 in complex with CRISPR RNA, Nature 532 (7600) (2016) 522.
[68] J. Jiao, C.J. Duan, L. Xue, Y.F. Liu, W.H. Sun, Y. Xiang, DNA nanoscaffold-based SARS-CoV-2 detection for COVID-19 diagnosis, Biosens, Bioelectron 167 (2020), 112479.
[69] X. Ding, K. Yin, Z.Y. Li, R.V. Lalla, E. Ballesteros, M.M. Sfeir, C.C. Liu, Ultrasensitive and visual detection of SARS-CoV-2 using all-in-one dual CRISPR-Cas12a assay, Nat. Commun. 11 (1) (2020) 4711.
[70] X. Zhu, X.X. Wang, S.J. Li, W.K. Luo, X.P. Zhang, C.Z. Wang, Q. Chen, S.Y. Yu, J. Tai, Y. Wang, Rapid, ultrasensitive, and highly specific diagnosis of COVID-19 by CRISPR-based detection, ACS Sens 6 (3) (2021) 881–888.
[71] J.P. Broughton, X.D. Deng, G.X. Yu, C.L. Fasching, V. Servellita, J. Singh, X. Miao, J.A. Streithorst, A. Granados, A. Sotomayor-Gonzalez, K. Zorn, A. Gopez, E. Hsu, W. Gu, S. Miller, C.-Y. Pan, H. Guevara, D.A. Wadford, J.S. Chen, C.Y. Chiu, CRISPR-Cas12-based detection of SARS-CoV-2, Nat. Biotechnol. 38 (7) (2020) 870–874.
[72] M. Patchsung, K. Jantarug, A. Pattama, K. Aphicho, S. Suraritdechachai, P. Meesawat, K. Sappakhaw, N. Leelahakorn, T. Ruenkam, T. Wongsatit, N. Athipanyasilp, B. Eiamthong, B. Lakkanasirorat, T. Phoodokmai, N. Niljianskul, D. Pakotiprapha, S. Chanarat, A. Homchan, R. Tinikul, P. Kamutira, K. Phiwkaow, S. Soithongcharoen, C. Kantiwiriyawanitch, V. Pongsupasa, D. Trisrivirat, J. Jaroensuk, T. Wongnate, S. Maenpuen, P. Chaiyen, S. Kamnerdnakta, J. Swangsri, S. Chuthapisith, Y. Sirivatanauksorn, C. Chaimayo, R. Sutthent, W. Kantakamalakul, J. Joung, A. Ladha, X. Jin, J.S. Gootenberg, O.O. Abudayyeh, F. Zhang, N. Horthongkham, C. Uttamapinant, Clinical validation of a Cas13-based assay for the detection of SARS-CoV-2 RNA, Nat. Biomed. Eng. 4 (12) (2020) 1140–1149.
[73] K.H. Ooi, M.M. Liu, J.W.D. Tay, S.Y. Teo, P. Kaewsapsak, S.Y. Jin, C.K. Lee, J. W. Hou, S. Maurer-Stroh, W.S. Lin, B. Yan, G. Yan, Y.-G. Gao, M.H. Tan, An engineered CRISPR-Cas12a variant and DNA-RNA hybrid guides enable robust and rapid COVID-19 testing, Nat. Commun. 12 (1) (2021) 1739.
[74] M. Alafeef, K. Dighe, P. Moitra, D. Pan, Rapid, ultrasensitive, and quantitative detection of SARS-CoV-2 using antisense oligonucleotides directed electrochemical biosensor chip, ACS Nano 14 (12) (2020) 17028–17045.
[75] W. Heo, K. Lee, S. Park, K.A. Hyun, H.I. Jung, Electrochemical biosensor for nucleic acid amplification-free and sensitive detection of severe acute respiratory syndrome coronavirus 2 (SARS-CoV-2) RNA via CRISPR/Cas13a trans-cleavage reaction, Biosens. Bioelectron. 201 (2022), 113960.
[76] L. Kashefi-Kheyrabadi, H.V. Nguyen, A. Go, C. Baek, N. Jang, J.M. Lee, N.H. Cho, J. H. Min, M.H. Lee, Rapid, multiplexed, and nucleic acid amplification-free detection of SARS-CoV-2 RNA using an electrochemical biosensor, Biosens. Bioelectron. 195 (2022), 113649.